Biosensors and Bioelectronics 176 (2021) 112954

Contents lists available at ScienceDirect

Biosensors and Bioelectronics

journal homepage: http://www.elsevier.com/locate/bios

Cas12a-based electrochemiluminescence biosensor for target amplification-free DNA detection

Peng-Fei Liu [a,1], Kai-Ren Zhao [a,1], Zhi-Jun Liu [a,1], Li Wang [a,*], Shu-Ying Ye [b], Guo-Xi Liang [b,**]

[a] School of Pharmacy, Jiangsu University, Zhenjiang, 212013, China
[b] School of the Environment and Safety Engineering, Jiangsu University, Zhenjiang, 212013, China

ARTICLE INFO

Keywords:
Electrochemiluminescence
Cas12a
Biosensor
L-Methionine stabilized Gold nanoclusters
Target amplification-free

ABSTRACT

CRISPR/Cas system have drawn increasing attention in accurate and sensitive nucleic acids detection. Herein, we reported a novel Cas12a-based electrochemiluminescence biosensor for target amplification-free human papilloma virus subtype (HPV-16) DNA detection. During this detection process, Cas12a employed its two-part recognition mechanism to improve the specificity and trans-cleavage capability to achieve signal amplification, while L-Methionine stabilized gold nanoclusters (Met-AuNCs) were served as high-efficiency ECL emitters to achieve ECL signal transition. Given the unique combination of Cas12a with ECL technique, the detection limit was determined as 0.48 pM and the whole detection could be completed within 70 min. We also validated the practical application of the proposed biosensor by using undiluted human blood samples, which gives impetus to the design of new generations of CRISPR/Cas detection system beyond the traditional ones with ultimate applications in sensing analysis and diagnostic technologies.

1. Introduction

Accurate and sensitive nucleic acids detection is always of great importance in disease assessment and plays a crucial role in early clinical diagnosis (Gerasimova and Kolpashchikov, 2014; Urdea et al., 2006; Wu and Qu, 2015). CRISPR/Cas systems, which are components of bacterial immune systems (Horvath and Barrangou, 2010), as emerging and powerful tools have engaged great awareness in genome editing (Wang et al., 2013), bioengineering (English et al., 2019), and diagnostics (Gootenberg et al., 2017). On the base of their unique tunable nuclease activities, a series of highly sensitive CRISPR/Cas-based biosensor have been developed for nucleic acids detection such as Cas9 (Hajian et al., 2019; Liu et al., 2016; Zhou et al., 2018), SHERLOCK (Cas13a) (Gootenberg et al., 2017, 2018), DETECTR (Cas12a) (Chen et al., 2018a), CDetection (Cas12b) (Teng et al., 2019) and Cas14-DETECTR (Harrington et al., 2018). Especially, Cas12a and Cas13a have collateral promiscuous DNase or RNase activity upon target DNA/RNA recognition, showing enhanced sensitivity compared with the traditional methods (Kellner et al., 2019; Li et al., 2018a, 2018b; Peng et al., 2020), holding a great promise in developing next-generation diagnostic biosensors (Li et al., 2019a). The combination of Cas12a and Cas13a with other detection methods has been rapidly developed from fluorescence to electrochemistry (Bruch et al., 2019a; Dai et al., 2019; Zhang et al., 2020) and colorimetric methods (Li et al., 2019b; Yuan et al., 2020), where the CRISPR/Cas systems serving as a programmable and integrated biomolecular component can achieve accurate recognition and amplified signal transduction for biosensing (Dai et al., 2020).

Electrochemiluminescence (ECL), the marriage of electrochemistry and chemiluminescence, has drawn arising attention in bioanalysis and clinical diagnostics (Guo et al., 2018; Maar et al., 2019; Peng et al., 2019), due to the excellent properties such as simple device requirement, low background noise, high sensitivity, and wide dynamic range (Liu et al., 2015; Peng et al., 2019; Richter, 2004; Yan et al., 2019). Given these fascinating potentials, ECL may be an appropriate alternative technology to combine with CRISPR/Cas system for biosensing. However, to the best our knowledge, only one research paper has been reported on the CRISPR/Cas-based ECL biosensor (Zhou et al., 2020). Although a LOD of 1×10^{-15} M for miR-17 was achieved in that work, it still suffers from the high background because the emitter [Ru

* Corresponding author.
** Corresponding author.
E-mail addresses: wangjill@126.com (L. Wang), gxliang@ujs.edu.cn (G.-X. Liang).
[1] These authors contributed equally to this work.

https://doi.org/10.1016/j.bios.2020.112954
Received 8 October 2020; Received in revised form 16 December 2020; Accepted 28 December 2020
Available online 1 January 2021

$(phen)_2dppz]^{2+}$ could be noncovalently attach to dsDNA even without the target molecular. Therefore, a mean to reduce the background of CRISPR-based ECL sensor is necessary. Moreover, as we all know, Ru-complexes are relatively expensive and have large steric hindrance, which limits the immobilization capacity to some extent and reduces the sensitivity (Yao et al., 2020). It is still necessary to find cost-effective ECL materials in CRISPR-based ECL biosensors.

Over decades, a variety of efficient emitters were successively developed such as metal nanoclusters (Wang et al., 2016; Yang et al., 2019), carbon nitride nanosheets (Chen et al., 2018b) and emerging perovskite nanocrystals (Cai et al., 2018; Tan et al., 2017). Among these emitters, gold nanoclusters (AuNCs) as emerging green nanomaterials are arising from increasing attention in the ECL field owing to their excellent biocompatibility, distinctive optical, and electrochemical properties (Xie et al., 2009; Yao et al., 2015, 2017), which have been extensively employed for ECL-based assays (Zhou et al., 2019; Jia et al., 2020).

Taking as-mentioned into consideration, herein, a Cas12a-based ECL biosensor was constructed for target amplification-free DNA detection, where Cas12a employed its two-part recognition mechanism to improve the specificity, and trans-cleavage capability to achieve signal amplification, while L-Methionine stabilized gold nanoclusters (Met-AuNCs) were served as high-efficiency ECL emitters to achieve ECL signal transition. In this detection procedure, human papilloma virus subtype (HPV-16), which is critical to carcinogenesis (Mirabello et al., 2017; Dai et al., 2019), was recruited as the target model. Initially, Met-AuNCs were modified on the surface of electrode to obtain an original signal. Ferrocene-tagged thiolated single-strand DNA (SH-ssDNA-Fc) as non-specific ssDNA was subsequently tethered on the surface of Met-AuNCs to quench their emission. When target HPV-16 DNA was presented, with the assistance of two-part recognition system, Cas12a was activated and possessed trans-cleavage ability on non-specific ssDNA, leading to the indiscriminate cleavage of SH-ssDNA-Fc into short fragments. Through recording the recovered ECL signal under different concentrations of target HPV-16 DNA, the quantitative detection could be achieved with a detection limit of 0.48 pM, which is superior to most nucleic acid amplification-free CRISPR-based works. Furthermore, this biosensor exhibited desirable performance in detecting HPV-16 DNA in undiluted human blood samples. Moreover, due to the programmability of the sequence of crRNA, the biosensor can detect any other DNA biomarker as an all-purpose detection strategy. It is no exaggeration to say that the Cas12a-based ECL biosensor lays a solid foundation for further development of CRISPR/Cas-based ECL biosensors.

2. Experimental section

2.1. Materials and reagents

Cas12a endonuclease separated from Lachnospiraceae bacterium ND2006 was purchased from New England Biolabs (MA, USA). CRISPR RNA (crRNA) was brought from Gene Pharma (Shanghai, China). L-Methionine (Met) and hydrogen tetrachloroaurate (III) trihydrate ($HAuCl_4{\cdot}3H_2O$) were bought from Aladdin Chemistry Co Ltd. (Shanghai, China). Triethylamine (TEA) was purchased from Sinopharm Chemical Reagent Co., Ltd. (Shanghai, China). 6-Mercapto-1-hexanol (MCH) and tris(2-carboxyethy) phosphine hydrochloride (TCEP) were obtained from Sigma-Aldrich (St Louis, USA). All DNA oligonucleotides were synthesized and purified from Sangon Biotech Co., Ltd. (Shanghai, China) and sequences of them were listed in Table S1. RNase-free water was employed as the solvent throughout the experiment. Tris-HCl buffer (pH = 7.9, 10 mM Tris-HCl, 50 mM NaCl, 20 mM $MgCl_2$ and 100 μg/mL BSA) was served as the solution medium of oligonucleotides and CRISPR/Cas12a duplex. Phosphate buffer saline (PBS, 0.1 M) (K_2HPO_4–KH_2PO_4–KCl) containing 0.2 M TEA was used as the ECL working solution with the final pH of 11. All chemical reagents were of analytical grade.

2.2. Apparatus

Transmission electron microscope (TEM) image was obtained from a JEM-2100 (JEOL, Japan) with the accelerating voltage setting at 100 kV. UV–visible spectrum was obtained from UV-2400 (Shimadzu, Japan). A homemade ECL detection device, containing a model CHI 660E workstation and an RFL-1 ultraweak chemiluminescence detector (Remax, China), was utilized to record the corresponding ECL signal. Electrochemical impedance spectroscopy (EIS) was measured in 5 mM $[Fe(CN)_6]^{3-/4-}$ solution containing 0.1 M KCl by using a CHI 660E workstation (Shanghai, China) with a classical three-electrode arrangement as follows: a modified gold electrode (GE, $\Phi = 3$ mm) as working electrode, a platinum wire as counter electrode and an Ag/AgCl as reference electrode, respectively. The equipment needed to run the Cas12a-ECL protocol can be seen in Fig. S1.

2.3. Synthesis of Met-AuNCs

Met-AuNCs were prepared according to the reported method with little modification (Peng et al., 2019). In brief, 4 mL Met (0.1 M), 0.6 mL NaOH (0.5 M) and 0.4 mL $HAuCl_4$ solution (20 mg/mL) were mixed thoroughly. Thereafter, the mixture was allowed to react at 37 °C for 6 h until a faint yellow solution was observed. Subsequently, 0.5 mL H_2SO_4 (1 M) was utilized to refine and precipitate the as-prepared Met-AuNCs. After a centrifugation process with 6000 rpm for 2 min, the precipitated Met-AuNCs were gathered and washed by 5 mL H_2SO_4 (0.1 M) for three times. Ultimately, the Met-AuNCs were rinsed and dispersed in 5 mL RNase-free water. The resultant Met-AuNCs solution was diluted for 10 times using RNase-free water and stored in the dark at 4 °C for later use. The prepared Met-AuNCs was characterized in Supplementary Information (Fig. S2).

2.4. Modification of the ECL biosensing electrode

Prior to use, the bare GE was burnished by 0.3 and 0.05 μm alumina powder to form a mirror-like smoothness. Then, the GE was ultrasonicated with ethanol and RNase-free water respectively, and further treated with an electrochemically cleaned method by scanning in 0.5 M H_2SO_4 until a stable voltammetric peak was observed. Thereafter, 10 μL as-prepared Met-AuNCs was cast onto the electrode to form Met-AuNCs/GE and dried under a nitrogen flow. Afterwards, 10 μL SH-ssDNA-Fc (4 μM), which was pretreated with 10 mM TCEP to reduce disulfide bonds, was introduced on the as-modified GE and incubated at a humid environment overnight. After washing with RNase-free water and the modified GE was immediately immersed into 1 mM MCH to passivate the electrode and replace loosely tethered SH-ssDNA-Fc to form a highly-aligned surface. Finally, the as-modified GE was thoroughly rinsed by RNase-free water and stored at 4 °C for further experiment.

2.5. Target detection protocol

Cas12a-crRNA duplex was prepared in a buffer prepared by RNase-free water containing 10 mM Tris-HCl, 50 mM NaCl, 20 mM $MgCl_2$ and 100 μg/mL BSA with a pH of 7.9 (Dai et al., 2019). Cas12a-crRNA duplex (50 nM, final concentration) was initially assembled and incubated at ambient temperature for 10 min. Afterwards, 5 μL different concentration of target HPV-16 DNA (1 pM, 5 pM, 10 pM, 50 pM, 100 pM, 500 pM, 1 nM, 10 nM) was introduced into 20 μL Cas12a-crRNA duplex solution and incubated for another 10 min. Subsequently, 15 μL resulted solution was introduced on the surface of the as-modified GE (MCH/SH-ssDNA-Fc/Met-AuNCs/GE) and incubated for 60 min. Finally, after washing with RNase-free water, the electrode was measured in ECL testing solution with the potential ranging from 0 to +1.0 V, scan rate of 100 mV/s and photomultiplier tube (PMT) of 800 V, respectively.

3. Results and discussion

3.1. Principle of the Cas12a-based ECL biosensor

The principle of the Cas12a-based ECL biosensor was illustrated in Scheme 1. Initially, Met-AuNCs were served as the substrate emitters and were dropped on the GE surface to obtain an original ECL signal. Thereafter, SH-ssDNA-Fc, which was pretreated with TCEP to cut off disulfide bonds, was introduced on the electrode to quench the emission of Met-AuNCs. In the presence of target DNA, Cas12a-crRNA duplex identified target DNA through two-part recognition mechanism, and the trans-cleavage ability of Cas12a was activated and indiscriminately cleaved the non-specific SH-ssDNA-Fc, leading to the recovery of Met-AuNCs emission. Through recording the ECL signal change under different concentrations of target DNA, the quantificational detection was achieved.

3.2. Feasibility analysis of the Cas12a-based ECL biosensor

To validate the recognition and trans-cleavage ability of CRISPR/Cas12a system, polyacrylamide gel electrophoresis (PAGE) was firstly carried out. To make the result of clearer, a 40 nt ssDNA was employed as the non-specific ssDNA. As depicted in Fig. 1A, only the coexistence of Cas12a and crRNA could specifically recognize target DNA, subsequently triggering the cleavage of non-specific ssDNA (lane 4). Once component of the Cas12a-crRNA duplex was absent, no recognition and cleavage occurred and there is no impact on target DNA and ssDNA (lane 1 and lane 2). Similarly, when both Cas12a and crRNA were inexistent, there was also no significant impact on target DNA and ssDNA (lane 3). Furthermore, in the absence of target DNA, Cas12a-crRNA duplex was inactive and could not possess the trans-cleavage ability on non-specific ssDNA (lane 5). The PAGE result could serve as a forceful evidence for recognition and trans-cleavage ability of Cas12a system.

ECL measurement was implemented to access the trans-cleavage ability of Cas12a. The as-modified electrode (MCH/SH-ssDNA-Fc/Met-AuNCs/GE) was treated with a series of mixtures respectively (crRNA-target, Cas12a-target, target, and Cas12a-crRNA-target) and incubated at 37 °C for 1 h. After rinsing with RNase-free water, the electrode was measured in ECL testing solution. As depicted in Fig. 1B, only the mixture containing Cas12a, crRNA and target could form Cas12a-crRNA-target triplex and activate the trans-cleavage ability of Cas12a, leading to the cleavage of the SH-ssDNA-Fc and corresponding recovery of Met-AuNCs emission, while all of other mixtures showed negligible impacts on the SH-ssDNA-Fc owing to the incapable trans-cleavage ability of Cas12a. Both the results of PAGE and ECL measurement corroborated the activation conditions for the trans-cleavage ability of Cas12a, indicating the feasibility of the Cas12a-based ECL biosensor.

3.3. Characterization of the Cas12a-based ECL biosensor

The stepwise modification of the Cas12a-based ECL biosensor was firstly investigated by ECL measurement. As shown in Fig. 2A, a negligible ECL signal was observed from bare GE (curve a). Afterwards, the Met-AuNCs were modified on the electrode surface, leading to a considerable ECL signal (curve b). When a mass of SH-ssDNA-Fc were introduced on the GE surface, a sharp decrease of the ECL signal could be seen due to a quenching effect on the ECL emission of Met-AuNCs (curve c). Finally, upon the addition of activated Cas12a, the SH-ssDNA-Fc was cleaved into fragments and the Fc tagging at the 3' terminus was released, resulting in the recovery of the ECL emission of Met-AuNCs (curve d), which demonstrates the successfully stepwise modification of the Cas12a-based ECL biosensor.

Electrochemical impedance spectroscopy (EIS), as a conventional common method utilized to access the modification process of the electrode interface (Yang et al., 2017), was further employed to investigate the modification process of the Cas12a-based ECL biosensor. And the semicircle diameter is directly related to electron transfer resistance (Ret) (Peng et al., 2016; Zhang et al., 2018). As displayed in Fig. 2B, a teeny semicircle diameter was observed in bare GE (curve a). Then, only a small increase of semicircle diameter could be seen when the Met-AuNCs was immobilized on GE surface (curve b). Later, with the addition of SH-ssDNA-Fc and MCH, the value of semicircle diameter further increased owing to a trade-off between the negative charged DNA, nonconductive MCH and excellent electronic conductivity of Fc (curve c) (Xu et al., 2019). Ultimately, when the modified GE was treated with activated Cas12a, a remarkable increase of semicircle diameter was revealed due to the cleavage of SH-ssDNA-Fc and the releasing of conductive Fc (curve d). Both the results of ECL and EIS validated the desirable fabrication of Cas12a-based ECL biosensor.

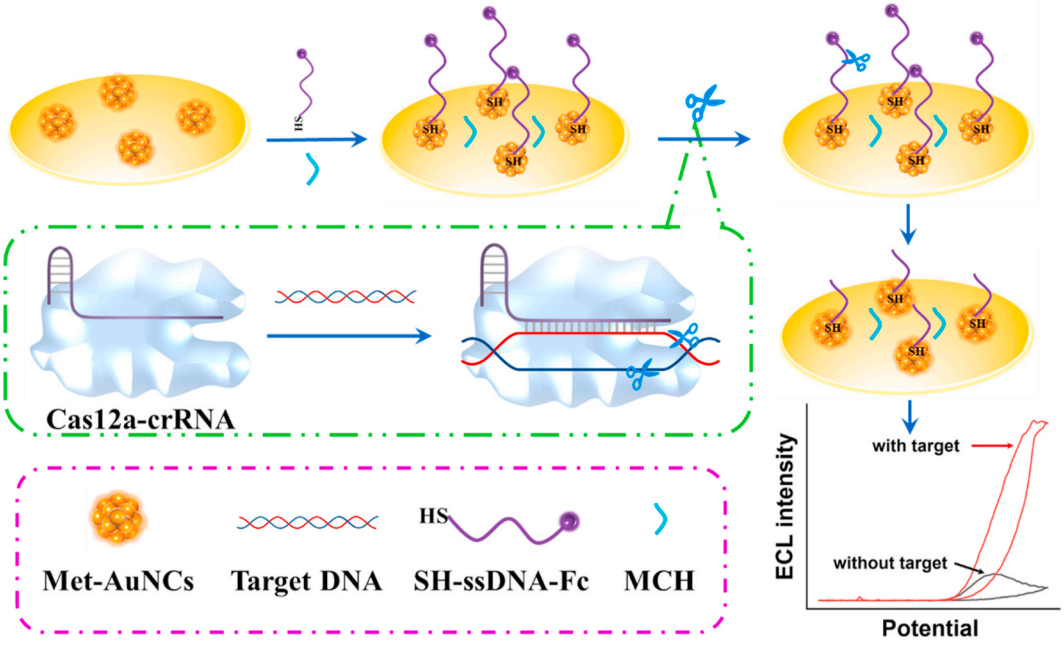

Scheme 1. The schematic diagram of the Cas12a-based ECL biosensor for target HPV-16 DNA detection.

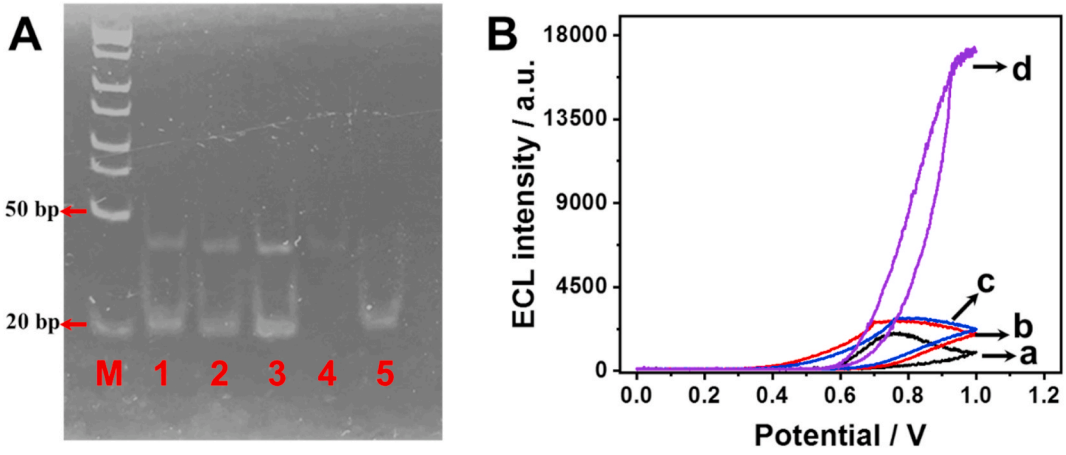

Fig. 1. (A) PAGE analysis of different samples. Lane 1: crRNA + target + ssDNA, Lane 2: Cas12a + target + ssDNA, Lane 3: target + ssDNA, Lane 4: Cas12a + crRNA + target + ssDNA, Lane 5: Cas12a + crRNA + ssDNA. (B) ECL analysis of different samples. (a) crRNA + target, (b) Cas12a + target, (c) only target, and (d) Cas12a + crRNA + target. Concentration of every component used in PAGE and ECL analysis, Cas12a: 50 nM, crRNA: 50 nM, target: 100 nM, ssDNA: 4 μM.

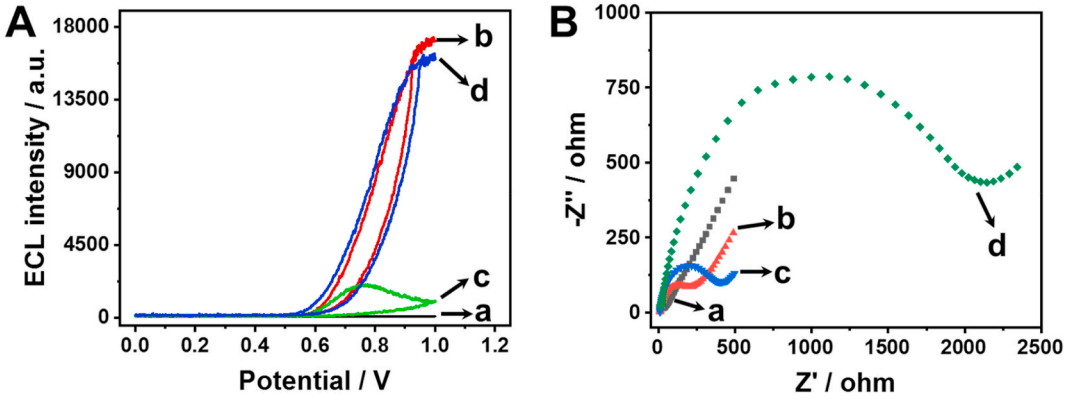

Fig. 2. ECL (A) and EIS (B) characterizations of the stepwise procedure of electrode: (a) bare GE, (b) Met-AuNCs/GE, (c) MCH/SH-ssDNA-Fc/Met-AuNCs/GE, and (d) MCH/SH-ssDNA-Fc/Met-AuNCs/GE treated with Cas12a-crRNA-target triplex. For EIS analysis, 5 mM $[Fe(CN)_6]^{3-/4-}$ solution containing 0.1 M KCl was used. The corresponding parameters were set as follows: initial potential of 0.20 V, amplitude of 0.005 V, frequency ranging from 10^{-1}–10^4 Hz, respectively.

3.4. Optimization of the conditions

To obtain the best performance of the Cas12a-based ECL biosensor, some significant factors were successively optimized including the concentrations of Met-AuNCs, coreactant (TEA), SH-ssDNA-Fc and Cas12a-crRNA duplex, as well as the trans-cleavage time of Cas12a on SH-ssDNA-Fc. First, the concentration of ECL emitter Met-AuNCs was optimized, and 10-fold diluted Met-AuNCs was selected (Fig. S3). The concentration of coreactant (TEA), which is closely associated with the ECL properties of Met-AuNCs, was next investigated. As seen in Fig. 3A, the ECL intensity of Met-AuNCs increased remarkably with the continuous addition of TEA concentration from 0.05 to 0.2 M and reached the peak at 0.2 M. Thusly, the optimized concentration of TEA was selected as 0.2 M to achieve an optimal ECL property of Met-AuNCs. In addition, the concentration of SH-ssDNA-Fc, which is correlated with the quenching effect to Met-AuNCs, was also evaluated. The ECL intensity gradually decreased when the concentration of Fc-labeled ssDNA increased from 0 to 4 μM and tended to a platform (Fig. 3B). Hence, 4 μM Fc-labeled ssDNA was chosen as the appropriate experimental condition. In addition, the quenching effect of 4 μM Fc-labeled ssDNA on Met-AuNCs at different concentrations was also studied. The results showed that the best quench was obtained for 10-fold diluted Met-AuNCs, which was quenched about 89% (Fig. S3). To obtain the best trans-cleavage ability of Cas12a, the concentration of Cas12a-crRNA duplex as another interrelated factor was examined and the result ranging from 10 nM to 60 nM was exhibited in Fig. 3C. The ECL intensity increased continuously until an exceeded concentration was clearly observed at 50 nM, which was appointed as the applicable concentration of Cas12a-crRNA duplex. Furthermore, trans-cleavage time of Cas12a on SH-ssDNA-Fc was highly related to the performance of the Cas12a-based ECL biosensor, which was strictly studied from 20 min to 100 min. As displayed in Fig. 3D, the ECL intensity increased sharply before 60 min, following by a slight increase. To make sure the timeliness of the Cas12a-based ECL biosensor, the trans-cleavage time of Cas12a on SH-ssDNA-Fc was applied as 60 min for a suitable condition. Otherwise, pH of the testing solution was optimized at 11 (Fig. S4).

3.5. Detection of HPV-16 DNA with the Cas12a-based ECL biosensor

Under the optimal experimental conditions, the Cas12a-based ECL biosensor was utilized for target HPV-16 DNA assay. A series of different concentrations of HPV-16 DNA was introduced into Cas12a-crRNA duplex solution, respectively. Then, the solution was incubated at ambient temperature for 10 min to activate the trans-cleavage ability of Cas12a. Afterwards, the well-modified GE was treated with above solution, incubated for 60 min and measured in ECL testing solution. The Cas12a-ECL assay can be run in approximately 70 min. As depicted in Fig. 4A, a continuous increase of ECL intensity of Met-AuNCs was observed with the gradually addition of HPV-16 DNA ranging from 1 pM to 10 nM. And a good linear relationship between ECL intensity and

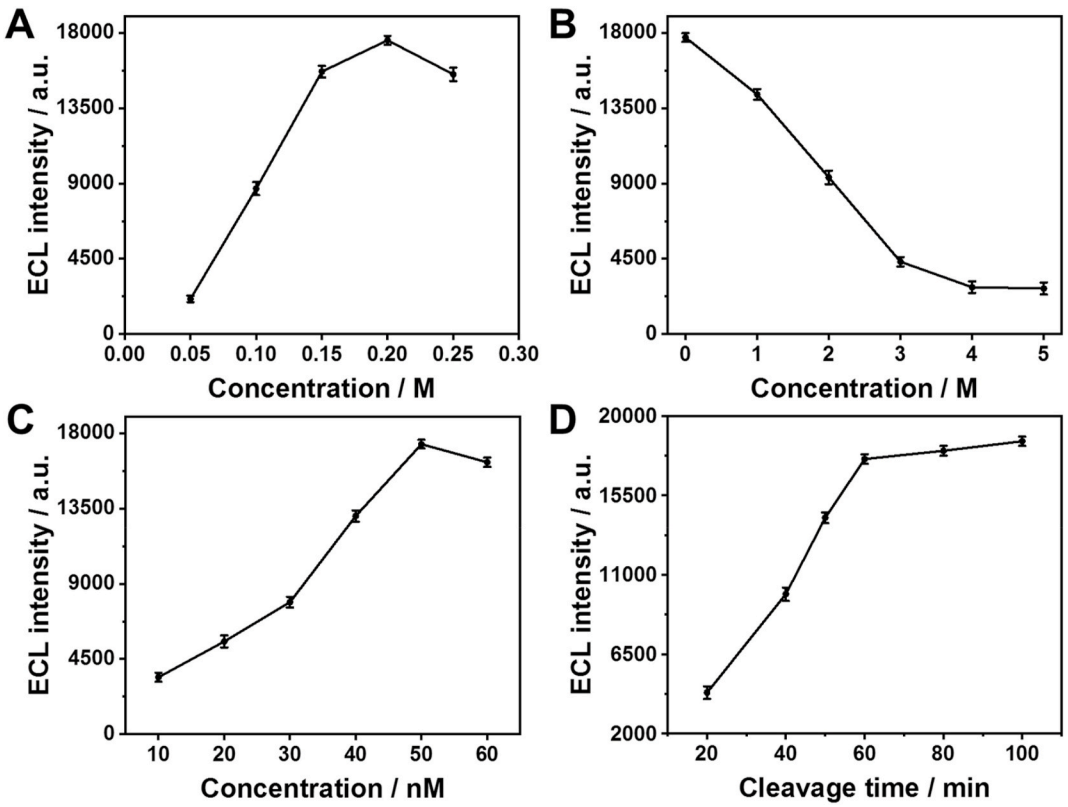

Fig. 3. Optimization of significant experimental conditions including concentration of coreactant TEA (A), SH-ssDNA-Fc (B), Cas12a/crRNA duplex (C), and cleavage time of Cas12a on SH-ssDNA-Fc (D). Error bar represents SD (n = 3).

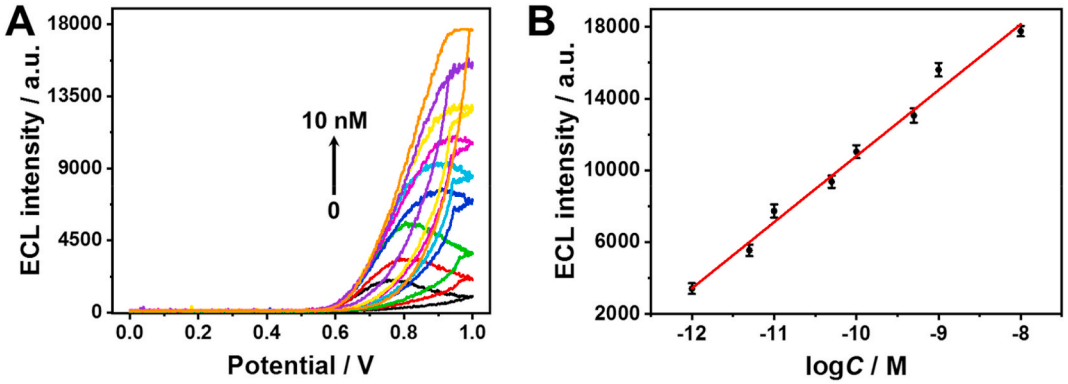

Fig. 4. (A). ECL-potential curve responding to 0, 1 pM, 5 pM, 10 pM, 50 pM, 100 pM, 500 pM, 1 nM, 10 nM target HPV-16 DNA. (B). Calibration curve between I and logarithmic concentration of target DNA. Error bar represents SD (n = 3).

logarithmic of target DNA concentration could be seen in Fig. 4B. The corresponding regression equation was $I = 3679 \log C + 47587$ ($R^2 = 0.9897$) with the determined limit of detection (LOD) as 0.48 pM (LOD $= k\ S_B/m$, the detailed calculation information can be seen in Supplementary Information and Fig. S5), which shows excellent performance on nucleic acids detection compared with published work (Table 1).

3.6. Specificity, reproducibility and availability of the Cas12a-based ECL biosensor

The specificity of the Cas12a-based ECL biosensor was evaluated by using HPV-18 DNA as interference agents. And the related results in Fig. 5A demonstrated the excellent specificity toward target HPV-16 DNA, which gave the credit to the brilliant recognize capability of Cas12a system. In addition, the reproducibility was also investigated by

Table 1
The comparison for amplification-free recent CRISPR-powered methods for nucleic acids detection.

Effector	Detecting technology	Detection ranges (M)	LOD (pM)	Reference
LbCas12a	Electrochemistry	10^{-11} to 10^{-7}	50	Dai et al. (2019)
LwaCas13a	Electrochemical Microfluidic	10^{-13} to 10^{-8}	10	Bruch et al. (2019a)
LbCas12a	Electrochemistry	5×10^{-13} to 10^{-7}	10	Zhang et al. (2020)
LbuCas13a	Colorimetric	5×10^{-13} to 10^{-8}	0.5	Yuan et al. (2020)
LbCas12a	Electrochemiluminescence	10^{-12} to 10^{-8}	0.48	This work

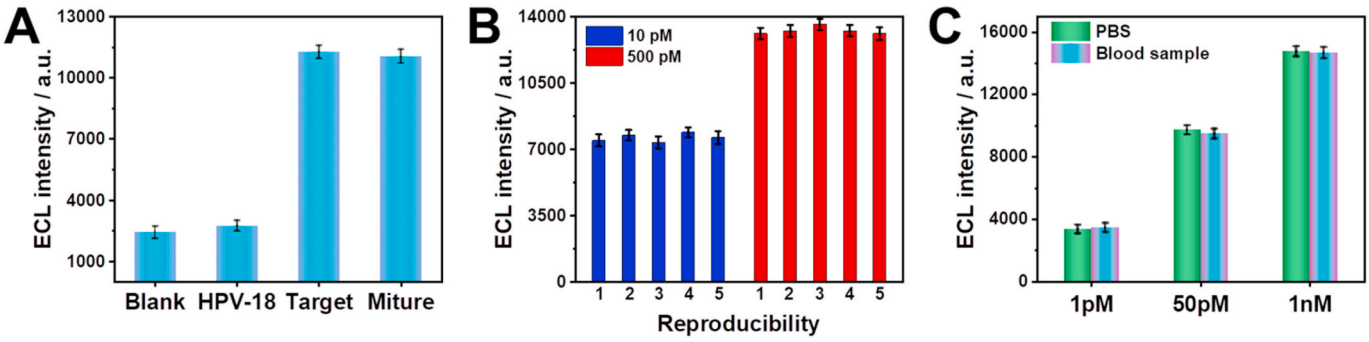

Fig. 5. (A) Specificity of the Cas12a-based ECL biosensor. Concentration of target (HPV-16) DNA and HPV-18 DNA: 50 pM. (B) Reproducibility of the ECL-CRISPR biosensor under different concentrations of target HPV-16 DNA. (C) Comparison of the performance of the Cas12a-based ECL biosensor for HPV-16 DNA in PBS and in undiluted human blood samples using the standard addition method. Error bar represents SD (n = 3).

fabricating five parallel measurements toward different concentrations of target DNA under the same experimental conditions (Fig. 5B), and a low relative standard deviation (RSD) of 1.4% and 0.7% was observed, indicating a superior reproducibility of the Cas12a-based ECL biosensor.

In order to validate the feasibility of the proposed ECL sensor, recovery tests based on the standard addition method were implemented in undiluted human blood samples. The recoveries ranged from 95.4–101.3%. Fig. 5C displayed the corresponding ECL intensity of different concentrations of target HPV-16 DNA in PBS and undiluted human blood samples under the same experimental conditions. The ECL intensity exhibited negligible difference. All these results suggested the proposed ECL sensor possessed promising potential in clinical diagnosis.

4. Conclusion

In summary, a novel Cas12a-based ECL biosensor was proposed for amplification-free HPV-16 DNA detection. Benefited from trans-cleavage capability of Cas12a system and high-efficiency ECL emission of Met-AuNCs, this biosensor showed high sensitivity for target HPV-16 detection with a LOD of 0.48 pM, which outperforms most nucleic acid amplification-free CRISPR-based works. More significantly, this Cas12a-based ECL biosensor provided high selectivity, the undiluted human blood samples detection was realized with satisfactory recoveries, which was thereby providing a potential application for point-of-care testing.

From the present study we provide a new combination of CRISPR/Cas system with ECL biosensor, and demonstrate its excellent performance for HPV-16 detection. However, as the researchers pointed out: one of the main disadvantages of CRISPR/Cas biosensing technology is the lack of multiplexing (Bruch et al., 2019b; Li et al., 2019a). Therefore, analyzing multiple analytes from a single sample will be the main problem need to be solved in the further work of CRISPR/Cas-ECL biosensors.

CRediT authorship contribution statement

Peng-Fei Liu: Conceptualization, Methodology, Project administration, Software, Visualization, Writing - original draft. **Kai-Ren Zhao:** Conceptualization, Data curation, Software, Validation, Visualization, Writing - review & editing. **Zhi-Jun Liu:** Writing - review & editing. **Li Wang:** Resources, Writing - review & editing, Supervision, Data curation, Funding acquisition. **Shu-Ying Ye:** Writing - review & editing. **Guo-Xi Liang:** Resources, Writing - review & editing, Supervision.

Declaration of competing interest

The authors declare that they have no known competing financial interests or personal relationships that could have appeared to influence the work reported in this paper.

Acknowledgement

This work was financially supported by National Natural Science Foundation of China (No. 21707053) and Senior Talent Foundation of Jiangsu University (No. 10JDG052, 10JDG038).

Appendix A. Supplementary data

Supplementary data to this article can be found online at https://doi.org/10.1016/j.bios.2020.112954.

References

Bruch, R., Baaske, J., Chatelle, C., Meirich, M., Madlener, S., Weber, W., Dincer, C., Urban, G.A., 2019a. CRISPR/Cas13a-powered electrochemical microfluidic biosensor for nucleic acid amplification-free miRNA diagnostics. Adv. Mater. 31, 1905311. https://doi.org/10.1002/adma.201905311.

Bruch, R., Urban, G.A., Dincer, C., 2019b. CRISPR/Cas powered multiplexed biosensing. Trends Biotechnol. 37, 791–792. https://doi.org/10.1016/j.tibtech.2019.04.005.

Cai, Z., Li, F., Xu, W., Xia, S., Zeng, J., He, S., Chen, X., 2018. Colloidal $CsPbBr_3$ perovskite nanocrystal films as electrochemiluminescence emitters in aqueous solutions. Nano Res 11, 1447–1455. https://doi.org/10.1007/s12274-017-1760-7.

Chen, J.S., Ma, E., Harrington, L.B., Da Costa, M., Tian, X., Palefsky, J.M., Doudna, J.A., 2018a. CRISPR-Cas12a target binding unleashes indiscriminate single-stranded DNase activity. Science 360, 436–439. https://doi.org/10.1126/science.aar6245.

Chen, S., Lv, Y., Shen, Y., Ji, J., Zhou, Q., Liu, S., Zhang, Y., 2018b. Highly sensitive and quality self-testable electrochemiluminescence assay of DNA methyltransferase activity using multifunctional sandwich-assembled carbon nitride nanosheets. ACS Appl. Mater. Interfaces 10, 6887–6894. https://doi.org/10.1021/acsami.7b17813.

Dai, Y., Somoza, R.A., Wang, L., Welter, J.F., Li, Y., Caplan, A.I., Liu, C.C., 2019. Exploring the trans-cleavage activity of CRISPR-Cas12a (cpf1) for the development of a universal electrochemical biosensor. Angew. Chem. Int. Ed. 58, 17399–17405. https://doi.org/10.1002/anie.201910772.

Dai, Y., Wu, Y., Liu, G., Gooding, J.J., 2020. CRISPR mediated biosensing toward understanding cellular biology and point-of-care diagnosis. Angew. Chem. Int. Ed. 59, 20754–20766. https://doi.org/10.1002/anie.202005398.

English, M.A., Soenksen, L.R., Gayet, R.V., de Puig, H., Angenent-Mari, N.M., Mao, A.S., Nguyen, P.Q., Collins, J.J., 2019. Programmable CRISPR-responsive smart materials. Science 365, 780–785. https://doi.org/10.1126/science.aaw5122.

Gerasimova, Y.V., Kolpashchikov, D.M., 2014. Enzyme-assisted target recycling (EATR) for nucleic acid detection. Chem. Soc. Rev. 43, 6405–6438. https://doi.org/10.1039/C4CS00083H.

Gootenberg, J.S., Abudayyeh, O.O., Kellner, M.J., Joung, J., Collins, J.J., Zhang, F., 2018. Multiplexed and portable nucleic acid detection platform with Cas13, Cas12a, and Csm6. Science 360, 439–444. https://doi.org/10.1126/science.aaq0179.

Gootenberg, J.S., Abudayyeh, O.O., Lee, J.W., Essletzbichler, P., Dy, A.J., Joung, J., Verdine, V., Donghia, N., Daringer, N.M., Freije, C.A., Myhrvold, C., Bhattacharyya, R.P., Livny, J., Regev, A., Koonin, E.V., Hung, D.T., Sabeti, P.C., Collins, J.J., Zhang, F., 2017. Nucleic acid detection with CRISPR-Cas13a/C2c2. Science 356, 438–442. https://doi.org/10.1126/science.aam9321.

Guo, W., Ding, H., Gu, C., Liu, Y., Jiang, X., Su, B., Shao, Y., 2018. Potential-resolved multicolor electrochemiluminescence for multiplex immunoassay in a single sample. J. Am. Chem. Soc. 140, 15904–15915. https://doi.org/10.1021/jacs.8b09422.

Hajian, R., Balderston, S., Tran, T., deBoer, T., Etienne, J., Sandhu, M., Wauford, N.A., Chung, J.Y., Nokes, J., Athaiya, M., Paredes, J., Peytavi, R., Goldsmith, B., Murthy, N., Conboy, I.M., Aran, K., 2019. Detection of unamplified target genes via CRISPR–Cas9 immobilized on a graphene field-effect transistor. Nat. Biomed. Eng. 3, 427–437. https://doi.org/10.1038/s41551-019-0371-x.

Harrington, L.B., Burstein, D., Chen, J.S., Paez-Espino, D., Ma, E., Witte, I.P., Cofsky, J.C., Kyrpides, N.C., Banfield, J.F., Doudna, J.A., 2018. Programmed DNA destruction by

miniature CRISPR-Cas14 enzymes. Science 362, 839–842. https://doi.org/10.1126/science.aav4294.
Horvath, P., Barrangou, R., 2010. CRISPR/Cas, the immune system of bacteria and archaea. Science 327, 167–170. https://doi.org/10.1126/science.1179555.
Jia, Y., Liu, S., Du, Y., Yang, L., Liu, X., Liu, L., Ren, X., Wei, Q., Ju, H., 2020. Intramolecular coreaction accelerated electrochemiluminescence of polypeptide-biomineralized gold nanoclusters for targeted detection of biomarkers. Anal. Chem. 92, 9179–9187. https://doi.org/10.1021/acs.analchem.0c01519.
Kellner, M.J., Koob, J.G., Gootenberg, J.S., Abudayyeh, O.O., Zhang, F., 2019. SHERLOCK: nucleic acid detection with CRISPR nucleases. Nat. Protoc. 14, 2986–3012. https://doi.org/10.1038/s41596-019-0210-2.
Li, S., Cheng, Q., Liu, J., Nie, X., Zhao, G., Wang, J., 2018a. CRISPR-Cas12a has both cis- and trans-cleavage activities on single-stranded DNA. Cell Res. 28, 491–493. https://doi.org/10.1038/s41422-018-0022-x.
Li, S., Cheng, Q., Wang, J., Li, X., Zhang, Z., Gao, S., Cao, R., Zhao, G., Wang, J., 2018b. CRISPR-Cas12a-assisted nucleic acid detection. Cell Discov 4, 20. https://doi.org/10.1038/s41421-018-0028-z.
Li, Y., Li, S., Wang, J., Liu, G., 2019a. CRISPR/Cas systems towards next-generation biosensing. Trends Biotechnol. 37, 730–743. https://doi.org/10.1016/j.tibtech.2018.12.005.
Li, Y., Mansour, H., Wang, T., Poojari, S., Li, F., 2019b. Naked-eye detection of grapevine red-blotch viral infection using a plasmonic CRISPR Cas12a assay. Anal. Chem. 91, 11510–11513. https://doi.org/10.1021/acs.analchem.9b03545.
Liu, W., Yu, H., Zhou, X., Xing, D., 2016. In vitro evaluation of CRISPR/Cas9 function by an electrochemiluminescent assay. Anal. Chem. 88, 8369–8374. https://doi.org/10.1021/acs.analchem.6b02338.
Liu, Z., Qi, W., Xu, G., 2015. Recent advances in electrochemiluminescence. Chem. Soc. Rev. 44, 3117–3142. https://doi.org/10.1039/C5CS00086F.
Maar, R.R., Zhang, R., Stephens, D.G., Ding, Z., Gilroy, J.B., 2019. Near-infrared photoluminescence and electrochemiluminescence from a remarkably simple boron difluoride formazanate dye. Angew. Chem. Int. Ed. 58, 1052–1056. https://doi.org/10.1002/anie.201811144.
Mirabello, L., Yeager, M., Yu, K., Clifford, G.M., Xiao, Y., Zhu, B., Cullen, M., Boland, J.F., Wentzensen, N., Nelson, C.W., RaineBennett, T., Chen, Z., Bass, S., Song, L., Yang, Q., Steinberg, M., Burdett, L., Dean, M., Roberson, D., Mitchell, J., Lorey, T., Franceschi, S., Castle, P.E., Walker, J., Zuna, R., Kreimer, A.R., Beachler, D.C., Hildesheim, A., Gonzalez, P., Porras, C., Burk, R.D., Schiffman, M., 2017. HPV16 E7 genetic conservation is critical to carcinogenesis. Cell 170, 1164–1174. https://doi.org/10.1016/j.cell.2017.08.001 e1166.
Peng, H., Huang, Z., Sheng, Y., Zhang, X., Deng, H., Chen, W., Liu, J., 2019. Pre-oxidation of gold nanoclusters results in a 66% anodic electrochemiluminescence yield and drives mechanistic insights. Angew. Chem. Int. Ed. 58, 11691–11694. https://doi.org/10.1002/anie.201905007.
Peng, K., Zhao, H., Xie, P., Hu, S., Yuan, Y., Yuan, R., Wu, X., 2016. Impedimetric aptasensor for nuclear factor kappa B with peroxidase-like mimic coupled DNA nano-ladders as enhancer. Biosens. Bioelectron. 81, 1–7. https://doi.org/10.1016/j.bios.2015.12.039.
Peng, S., Tan, Z., Chen, S., Lei, C., Nie, Z., 2020. Integrating CRISPR-Cas12a with a DNA circuit as a generic biosensor for amplified detection of microRNA. Chem. Sci. 11, 7362–7368. https://doi.org/10.1039/D0SC03084H.
Richter, M.M., 2004. Electrochemiluminescence (ecl). Chem. Rev. 104, 3003–3036. https://doi.org/10.1021/cr020373d.
Tan, X., Zhang, B., Zou, G., 2017. Electrochemistry and electrochemiluminescence of organometal halide perovskite nanocrystals in aqueous medium. J. Am. Chem. Soc. 139, 8772–8776. https://doi.org/10.1021/jacs.7b05073.
Teng, F., Guo, L., Cui, T., Wang, X.G., Xu, K., Gao, Q., Zhou, Q., Li, W., 2019. CDetection: CRISPR-Cas12b-based DNA detection with sub-attomolar sensitivity and single-base specificity. Genome Biol. 20, 132. https://doi.org/10.1186/s13059-019-1742-z.
Urdea, M., Penny, L.A., Olmsted, S.S., Giovanni, M.Y., Kaspar, P., Shepherd, A., Wilson, P., Dahl, C.A., Buchsbaum, S., Moeller, G., Burgess, D.C.H., 2006. Requirements for high impact diagnostics in the developing world. Nature 444, 73–79. https://doi.org/10.1038/nature05448.
Wang, H., Yang, H., Shivalila, C.S., Dawlaty, M.M., Cheng, A.W., Zhang, F., Jaenisch, R., 2013. One-step generation of mice carrying mutations in multiple genes by CRISPR/Cas-mediated genome engineering. Cell 153, 910–918. https://doi.org/10.1016/j.cell.2013.04.025.
Wang, T., Wang, D., Padelford, J.W., Jiang, J., Wang, G., 2016. Near-infrared electrogenerated chemiluminescence from aqueous soluble lipoic acid Au nanoclusters. https://doi.org/10.1021/jacs.6b03037, 138, 6380-6383.
Wu, L., Qu, X., 2015. Cancer biomarker detection: recent achievements and challenges. Chem. Soc. Rev. 44, 2963–2997. https://doi.org/10.1039/C4CS00370E.
Xie, J., Zheng, Y., Ying, J.Y., 2009. Protein-directed synthesis of highly fluorescent gold nanoclusters. J. Am. Chem. Soc. 131, 888–889. https://doi.org/10.1021/ja806804u.
Xu, Z., Chang, Y., Chai, Y., Wang, H., Yuan, R., 2019. Ultrasensitive electrochemiluminescence biosensor for speedy detection of microRNA based on a DNA rolling machine and target recycling. Anal. Chem. 91, 4883–4888. https://doi.org/10.1021/acs.analchem.9b00728.
Yan, H., Wei, X., Zhu, M.J., Cheng, Z., Lee, M., Lu, C., Xu, J.J., 2019. Aggregation-induced electrochemiluminescence of carboranyl carbazoles in aqueous media. Angew. Chem. Int. Ed. 58, 3162–3166. https://doi.org/10.1002/anie.201900283.
Yang, L., Zhang, B., Fu, L., Fu, K., Zou, G., 2019. Efficient and monochromatic electrochemiluminescence of aqueous-soluble Au nanoclusters via host–guest recognition. Angew. Chem. Int. Ed. 58, 6901–6905. https://doi.org/10.1002/anie.201900115.
Yang, Z., Lan, Q., Li, J., Wu, J., Tang, Y., Hu, X., 2017. Efficient streptavidin-functionalized nitrogen-doped graphene for the development of highly sensitive electrochemical immunosensor. Biosens. Bioelectron. 89, 312–318. https://doi.org/10.1016/j.bios.2016.09.026.
Yao, L.Y., Yang, F., Hu, G.B., Yang, Y., Huang, W., Liang, W.B., Yuan, R., Xiao, D.R., 2020. Restriction of intramolecular motions (RIM) by metal-organic frameworks for electrochemiluminescence enhancement: 2D Zr_{12}-adb nanoplate as a novel ECL tag for the construction of biosensing platform. Biosens. Bioelectron. 155, 112099. https://doi.org/10.1016/j.bios.2020.112099.
Yao, Q., Yu, Y., Yuan, X., Yu, Y., Zhao, D., Xie, J., Lee, J.Y., 2015. Counterion-assisted shaping of nanocluster supracrystals. Angew. Chem. Int. Ed. 54, 184–189. https://doi.org/10.1002/anie.201408675.
Yao, Q., Yuan, X., Fung, V., Yu, Y., Leong, D.T., Jiang, D., Xie, J., 2017. Understanding seed-mediated growth of gold nanoclusters at molecular level. Nat. Commun. 8, 927. https://doi.org/10.1038/s41467-017-00970-1.
Yuan, C., Tian, T., Sun, J., Hu, M., Wang, X., Xiong, E., Cheng, M., Bao, Y., Lin, W., Jiang, J., Yang, C., Chen, Q., Zhang, H., Wang, H., Wang, X., Deng, X., Liao, X., Liu, Y., Wang, Z., Zhang, G., Zhou, X., 2020. Universal and naked-eye gene detection platform based on the clustered regularly interspaced short palindromic repeats/Cas12a/13a system. Anal. Chem. 92, 4029–4037. https://doi.org/10.1021/acs.analchem.9b05597.
Zhang, D., Yan, Y., Que, H., Yang, T., Cheng, X., Ding, S., Zhang, X., Cheng, W., 2020. CRISPR/Cas12a-mediated interfacial cleaving of hairpin DNA reporter for electrochemical nucleic acid sensing. ACS Sens. 5, 557–562. https://doi.org/10.1021/acssensors.9b02461.
Zhang, L., Xiao, X., Xu, Y., Chen, D., Chen, J., Ma, Y., Dai, Z., Zou, X., 2018. Electrochemical assay for continuous monitoring of dynamic DNA methylation process. Biosens. Bioelectron. 100, 184–191. https://doi.org/10.1016/j.bios.2017.08.013.
Zhou, T., Huang, R., Huang, M., Shen, J., Shan, Y., Xing, D., 2020. CRISPR/Cas13a powered portable electrochemiluminescence chip for ultrasensitive and specific miRNA detection. Adv. Sci. 7, 1903661. https://doi.org/10.1002/advs.201903661.
Zhou, W., Hu, L., Ying, L., Zhao, Z., Chu, P.K., Yu, X., 2018. A CRISPR–Cas9-triggered strand displacement amplification method for ultrasensitive DNA detection. Nat. Commun. 9, 1–11. https://doi.org/10.1038/s41467-018-07324-5.
Zhou, Y., Chai, Y., Yuan, R., 2019. Highly efficient dual-polar electrochemiluminescence from Au_{25} nanoclusters: the next generation of multibiomarker detection in a single step. Anal. Chem. 91, 14618–14623. https://doi.org/10.1021/acs.analchem.9b03736.